Influence of CO_2 on Ultrasound-Induced Polymerizations in High-Pressure Fluids

M. W. A. Kuijpers, L. J. M. Jacobs, M. F. Kemmere, and J. T. F. Keurentjes
Process Development Group, Dept. of Chemical Engineering & Chemistry, Eindhoven University of Technology, P.O. Box 513, 5600 MB Eindhoven, The Netherlands

DOI 10.1002/aic.10464
Published online April 8, 2005 in Wiley InterScience (www.interscience.wiley.com).

A strong viscosity increase upon polymerization hinders cavitation and subsequent radical formation during an ultrasound-induced bulk polymerization. Ultrasound-induced radical polymerizations of methyl methacrylate (MMA) have been performed in CO_2-expanded MMA, as well as in bulk MMA. For this purpose, the phase behavior of CO_2/MMA systems has been determined. With temperature oscillation calorimetry, the influence of CO_2 on the viscosity and on the reaction kinetics of ultrasound-induced polymerizations of MMA has been studied. In contrast to polymerizations in bulk, this technique shows that a low viscosity is maintained during polymerization reactions in CO_2-expanded MMA. As a consequence, a constant or even increasing polymerization rate is observed when pressurized CO_2 is applied. © 2005 American Institute of Chemical Engineers *AIChE J,* 51: 1726–1732, 2005
Keywords: anti-solvent, cavitation, sonochemistry, calorimetry, radical polymerization, pressurized carbon dioxide

Introduction

Ultrasound-induced cavitation is known to enhance chemical reactions, as well as mass transfer at ambient temperatures and pressures. The chemical effects of cavitation arise from the extreme conditions in the bubble (10.000 K and 200 bar),[1] and the high strain rates outside the bubble (10^7 s^{-1})[2] generated upon implosion. Monomer molecules are dissociated by the high temperatures in the hot-spot, whereas polymer chains are fractured by the high strain rates.[3,4] These two effects lead to the formation of radicals, which can initiate a polymerization reaction. The majority of the radicals in an ultrasound-induced polymerization reaction originate from the polymer chains.[5] Since the radicals are generated *in situ* by ultrasound, no initiator or catalyst is required to perform an ultrasound-induced polymerization. An additional advantage of this technique is the intrinsic safe operation, because turning off the electrical power supply will immediately stop the radical formation and, consequently, the polymerization reaction.

An important factor during ultrasound-induced bulk polymerizations is the viscosity.[6] Upon reaction the long chains formed cause a drastic increase in the viscosity. A high viscosity hinders cavitation and, consequently, reduces the production rate of radicals.[7] In order to obtain a constant viscosity and, hence, a constant radical formation rate, an antisolvent for the polymer can be used. Two effects then lead to a lower liquid viscosity at a given polymer concentration. First, the gyration radius of a polymer chain in solution is smaller as compared to bulk systems, resulting in less entanglements of polymer chains. Second, at high polymer and/or antisolvent concentrations, the polymer precipitates from the solution. Consequently, the viscosity and, hence, the radical formation rate is expected to remain virtually constant. In this perspective, high-pressure CO_2 is an interesting medium as most monomers have a high solubility in CO_2, whereas it exhibits an antisolvent effect for most polymers.[8] However, up till now ultrasound is rarely studied at higher pressures, because in most cases a high static pressure hampers the growth of cavities. Recently, we have shown that cavitation is possible in pressur-

Correspondence concerning this article should be addressed to M. F. Kemmere at M.F.Kemmere@TUE.nl.

ized CO_2.[9] Unlike ordinary liquids, carbon dioxide has a high vapor pressure, which counteracts the static pressure. Cavitation is possible if the difference between the static and vapor pressure is smaller than the maximum acoustic pressure that can be applied.[10] Dense-phase fluids (with a strong emphasis on CO_2) provide possibilities for the development of sustainable polymer processes.[11,12] Additionally, ultrasound combined with high-pressure carbon dioxide allows the development of clean routes to produce polymers with specific properties, since no organic antisolvents are required.

In this work, the antisolvent effect of CO_2 on the ultrasound-induced polymerization of MMA is studied. First, phase equilibrium measurements are presented, which give the composition and the density of the CO_2/MMA system at different conditions. With these data, the liquid volume can be calculated, allowing for a proper comparison of the ultrasound-induced polymerization experiments. On the basis of a combination of phase equilibrium data and temperature oscillation calorimetry, the influence of the CO_2 fraction and polymer concentration on the viscosity of the solution is determined. With temperature oscillation calorimetry, the overall heat-transfer coefficient is measured, which can be coupled to the viscosity. Finally, the results of ultrasound-induced polymerization experiments are given, in which the influence of the CO_2 fraction on the produced polymer and the reaction kinetics is investigated.

Experimental Section

Phase equilibrium measurements

Phase equilibrium and density measurements were performed by two different techniques: using a high-pressure view-cell in combination with a CO_2-buffer cylinder and with a so-called Cailletet apparatus.[13]

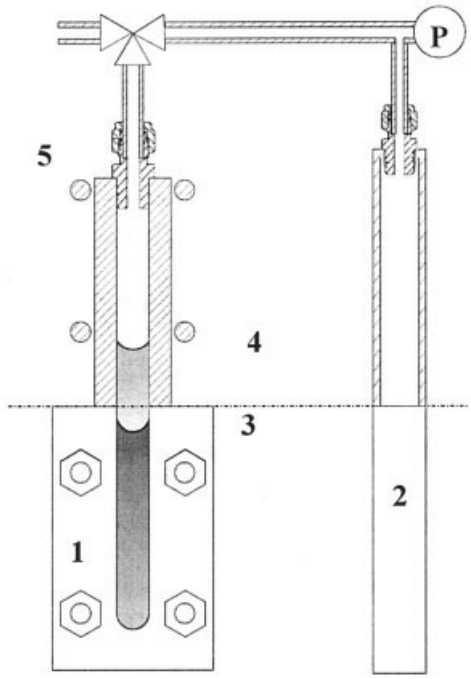

Figure 1. View-cell/CO_2-buffer cylinder apparatus, with (1) High-pressure view cell, (2) CO_2-buffer cylinder, (3) starting liquid volume, (4) expanded liquid volume, and (5) vacuum/CO_2.

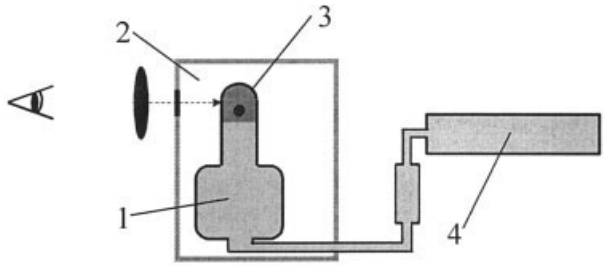

Figure 2. Cailletet apparatus, with: (1) mercury, (2) water, (3) sample, and (4) pressure system.

Figure 1. shows the setup of the view-cell and CO_2-buffer cylinder used for the equilibrium measurements. The whole apparatus was submerged in a water bath, which was thermostated within 0.1°C. The measurements in the view-cell were performed by filling the cell to a certain height with MMA (Merck) and evacuating all the air. After pressurization of the buffer cylinder with a known amount of CO_2 (grade 5.0, Hoekloos), it was connected with the view-cell. When equilibrium was reached, the expansion of the liquid was calculated from the rise of the meniscus. Using the known initial and final gas volume, as well as the pressure decrease in the system, the amount of CO_2 that dissolved in MMA was calculated with a modified Benedict-Webb-Rubin equation.[14] This equation calculates accurately the density of CO_2 as function of temperature and pressure. With the dissolved amount of CO_2 and the final liquid volume, the CO_2 fraction in the liquid phase and the liquid density were calculated. It was assumed that the amount of MMA in the gas phase is negligible.

In the Cailletet apparatus (Figure 2) the phase behavior of mixtures of constant composition can be determined visually by varying the pressure at constant temperature. A sample of the mixture with known composition was confined over mercury in the sealed top of a glass capillary tube. The static pressure on the CO_2/MMA system was increased until the vapor phase had disappeared. The pressure at which this occurs is the bubble point of the system. The mercury served as a sealing fluid and pressure transmitting fluid between the sample and the hydraulic system. The glass tube was thermostated with an accuracy of 0.01°C by circulating water of constant temperature.

Modeling phase equilibria

The Lee-Kessler-Plöcker (LKP) equation-of-state[15] is used to describe the phase behavior of the CO_2/MMA system. This equation-of-state applies to hydrocarbon systems, which include light gases, such as CO_2. The LKP-model uses pure component parameters, such as the critical temperature, the critical pressure and an acentric factor (ω), and a single binary interaction parameter. The LKP equation-of-state can be described in terms of compressibility factors (Z) in which *ref*1 is a reference fluid with an acentric factor of zero and *ref*2 is a fluid with a high acentric factor, that is, *n*-octane (Eq. 1). The compressibility factors of the reference fluids are a function of the reduced temperature and pressure of the mixture of interest. To obtain the mixture parameters, mixing rules are applied

using a binary interaction parameter for the critical temperature. The binary interaction parameter for LKP was determined by fitting the model to the experimental points at all temperatures

$$Z = Z_{ref1} + \frac{\omega_m - \omega_{ref1}}{\omega_{ref2} - \omega_{ref1}} (Z_{ref2} - Z_{ref1}) \quad (1)$$

Evaluation of the CO_2 anti-solvent effect

In ultrasound-induced polymerization reactions, the viscosity has a large influence on the radical formation rate. Therefore, it is important to monitor the viscosity during these reactions. By coupling the overall heat-transfer coefficient U to the viscosity of the reaction mixture, the influence of the CO_2-concentration on the viscosity of polymer solutions was determined

$$\frac{1}{U} = \frac{1}{h_i} + \frac{D_i}{2k_w} \ln \frac{D_0}{D_i} + \frac{1}{h_0} \frac{D_i}{D_0} \quad (2)$$

In Eq. 2, the heat-transfer coefficient is based on the inside area of the reactor, for which h_i and h_o represent the partial heat-transfer coefficients in the vessel and in the jacket, respectively; k_w stands for the thermal conductivity coefficient of the wall; D_i and D_o are the inner and outer diameter of the vessel.[16] The last two terms of Eq. 2 remain constant during a polymerization reaction, because the properties of the reactor wall and cooling liquid will not change during the experiments. Therefore, U is an indirect measure of the viscosity of the reaction mixture, since the empirical relation for the Nusselt number (Nu) as a function of the Reynolds (Re) and Prandtl number (Pr), can be applied to couple h_i to the viscosity. Equation 6, which is derived from Eqs. 3, 4 and 5, shows the influence of the viscosity on the overall heat-transfer coefficient. An increase in the viscosity (μ), thus, results in a decrease of the overall heat-transfer coefficient[17]

$$Nu = \frac{h_i D_i}{k_i} = 0.75\ \mathrm{Re}^{2/3}\mathrm{Pr}^{1/3} \quad (3)$$

Where the Reynolds and the Prandtl number stand for

$$\mathrm{Re} = \frac{\rho N D^2}{\mu} \quad (4)$$

$$\mathrm{Pr} = \frac{\mu C_p}{k_i} \quad (5)$$

$$\frac{1}{U} \sim \sqrt[3]{\mu} + \text{Constant} \quad (6)$$

The experiments to determine the influence of the CO_2 fraction and polymer concentration on the viscosity were performed in a commercially available reaction calorimeter RC1e (Figure 3, Mettler-Toledo GmbH, HP60 reactor, Switzerland). A detailed description of this equipment is given by Varela de la Rosa et al.[18] The reactor was filled with 1.5 L CO_2-expanded

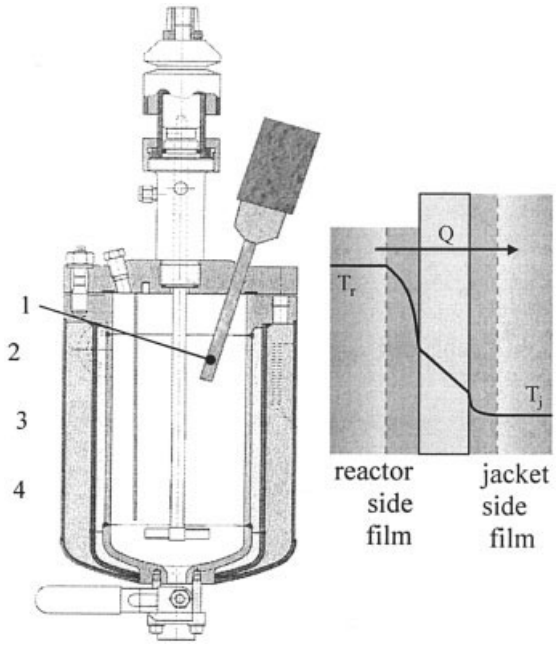

Figure 3. Reactor set-up and the resistances for heat transfer through the reactor wall, with (1) full-wave horn, (2) jacket, (3) reactor contents, and (4) impeller.

MMA, in which polymethyl methacrylate (PMMA, Aldrich), with a M_n of 141 kg/mol and a polydispersity of 2.2 was dissolved. A radical scavenger (1,1-diphenyl-2-picrylhydrazyl, Aldrich) was added to prevent polymerization. U was continuously calculated by temperature oscillation calorimetry[19,20] during the experiments with different polymer and CO_2-concentrations. The RC1e was operated in isothermal mode at 20°C, that is, the jacket temperature (T_j) of the reactor was automatically adjusted to keep the reactor temperature (T_r) constant.

Ultrasound-induced polymerizations

Ultrasound with a frequency of 20 kHz was produced using a Sonics and Materials VC750 ultrasonic generator. A 1/2-in. full-wave titanium probe was applied to couple the piezoelectric transducer to the liquid. To allow an accurate comparison, the total configuration of the reactor was exactly kept constant during all the experiments. The experiments were performed in the RC1e in isothermal mode at 20°C. Throughout the experiments the heat flow (Q) was calculated, based on the surface area of the reactor wall (A), the overall heat-transfer coefficient, and the difference between jacket and reactor temperature (Eq. 7). The ultrasound intensity (I_{US}), which is a measure of the acoustic pressure amplitude ($P_{A,\max}$, Eq. 8), was calculated by dividing the heat flow by the surface area of the ultrasound horn (A_{US})[10]

$$Q = UA(T_r - T_j) \quad (7)$$

$$P_{A,\max} = \sqrt{2\rho\nu \frac{Q}{A_{US}}} = \sqrt{2\rho\nu I_{US}} \quad (8)$$

For the polymerization reactions, the reactor was filled with 1.5 L CO_2-expanded MMA, in which 0.5 wt. % PMMA with a M_n of 141 kg/mol, and a polydispersity of 2.2 was dissolved. As the radicals in an ultrasound-induced polymerization reaction primarily originate from polymer chains and not from monomer molecules,[5] all polymerization experiments were performed with a small amount of added polymer in order to efficiently initiate the reaction. By the addition of polymer the inhibition period due to oxygen was minimized. The MMA was distilled under vacuum to remove the hydroquinone inhibitor before use. During the reaction CO_2 (grade 5.0) or argon (grade 5.0, Hoekloos) was bubbled through a 3 mm tube into the reaction mixture with a flow rate of 2.0 mL/s. These Ar or CO_2 bubbles served as nuclei for the cavities. Samples were taken during the experiments from which the conversion and the molecular weight distribution (MWD) of the polymer were obtained. Additionally, U was determined in time to monitor the viscosity. The MWDs were measured by gel permeation chromatography, calibrated against polystyrene standards. The molecular weight distributions of the PMMA samples were calculated with the appropriate Mark-Houwink parameters ($a = 0.719$ and $K = 9.44 * 10^{-5}$ m^3).[21]

Results and Discussion

In this study the influence of the CO_2 antisolvent effect on the viscosity and on the kinetics of an ultrasound-induced polymerization reaction have been studied. First, the phase behavior of the applied CO_2/MMA system has been determined and modeled. Next, the influence of the CO_2-concentration and polymer concentration on the liquid viscosity has been measured without polymerization. Finally, the antisolvent effect of CO_2 on the ultrasound-induced polymerization kinetics has been determined.

Phase behavior of the reaction mixture

The phase behavior of the CO_2-expanded MMA system is required to determine the influence of CO_2 on the viscosity during ultrasound-induced polymerization experiments. In Figure 4 several phase equilibrium measurements in the CO_2/MMA-system are presented. The phase equilibrium data of the experiments in the high-pressure view-cell (closed symbols) and in the Cailletet apparatus (open symbols), which are based on two different measurement principles, are in good agreement. The three isotherms in Figure 4 are obtained by modeling the bubble points with the LKP equation-of-state[15] with an interaction parameter of 1.08. With this temperature-independent interaction parameter, the measurements at 20°C, 30°C and 40°C are accurately modeled. In principle, the use of such a model also allows for extrapolation to higher CO_2 fractions.

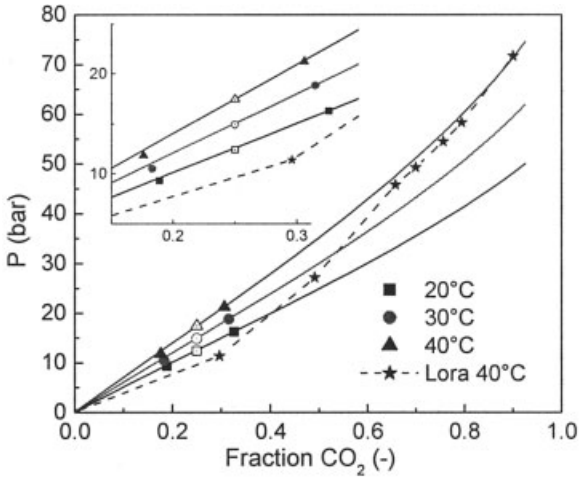

Figure 4. Measured bubble points of the CO_2/MMA system and the calculations based on the Lee-Kessler-Plöcker equation of state.

Open symbols are measurements with the Cailletet apparatus.

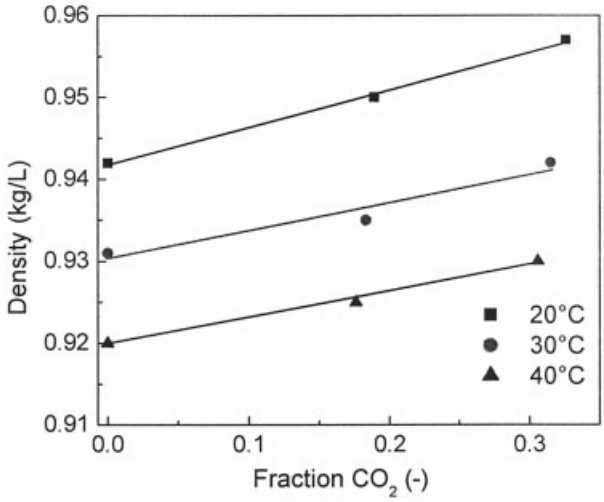

Figure 5. Density of the CO_2-expanded MMA system at 20°C, 30°C and 40°C.

Our measurements at 40°C as obtained in the two described apparatuses show substantially higher values at low CO_2 fractions as compared to the experimental data reported by Lora and McHugh.[22] However, the data from Lora and McHugh do coincide with the Lee-Kessler model at 40°C above a CO_2 fraction of 0.65. This deviation at low pressures probably originates from the plunger apparatus used by Lora and McHugh. This system is less accurate at low pressures caused by friction of the plunger, due to which a lower equilibrium pressure is observed at a given CO_2 fraction.

Subsequently, the density of the CO_2-expanded MMA system has been calculated from the view-cell experiments. The density increases when more CO_2 dissolves, see Figure 5, in which the lines show the trend. However, a reduction of the density is expected at higher CO_2 fractions as pure CO_2 at 20°C and 30°C has a density of 0.776 kg/L and 0.595 kg/L, respectively. This implies that the density is not a linear function between the two pure components. An increase in density does not imply that the MMA-phase does not expand. For instance, by applying 18 bar of CO_2 pressure at 20°C, the liquid volume increases by 20%. The slightly higher density at 18 bar is the result of the strong interaction between MMA and CO_2, due to which large amounts of CO_2 dissolve in MMA.

Anti-solvent effect of CO_2

The liquid viscosity has a major influence on the implosion velocity and, consequently, on the polymerization rate. To

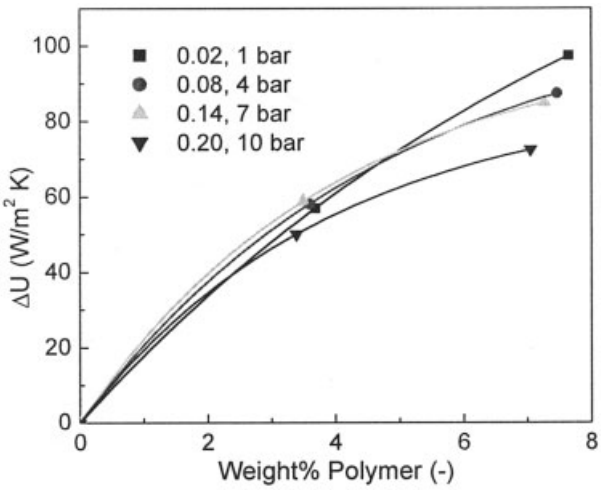

Figure 6. Heat-transfer coefficient difference as a function of the polymer weight percentage at different CO_2 fractions.

quantify the influence of the CO_2 fraction on the liquid viscosity, the overall heat-transfer coefficients are determined for polymer solutions in which no polymerization occurs. Figure 6 shows the influence of the polymer concentration (C_{pol}) and CO_2 fraction on U, and, consequently, on the liquid viscosity. The plotted difference (ΔU) is calculated by subtracting U with polymer ($U(C_{pol})$) from U without polymer ($U(0)$) at a given CO_2 fraction (Eq. 9). The curves in Figure 6 give the trend of the heat transfer decrease and, consequently, the viscosity increase (Eq. 6)

$$\Delta U = U(0) - U(C_{pol}) \tag{9}$$

At polymer concentrations above 4 weight percent, a distinct difference between the overall heat-transfer coefficients at different CO_2 fractions is obtained. This is a clear evidence for the antisolvent effect of CO_2. It is not a dilution effect due to the expansion of MMA, as this is taken into account by the calculation of the polymer concentration. The antisolvent effect at lower concentrations is not apparent, since the polymer coils start overlapping at a polymer concentration of approximately 4 weight percent. Moreover, the antisolvent effect is expected to be more distinct with higher molecular weight polymer as the chains will overlap at lower concentrations. In view-cell experiments of a solution of 7.5 wt. % PMMA in MMA at 13 bar CO_2 and 20°C, no second-phase (polymer phase) has been observed, which implies that the lower viscosity is due to the smaller gyration radius of the polymer chains, so that higher polymer concentrations or CO_2 fractions are required to induce precipitation of the polymer.

Polymerizations

The results of the ultrasound-induced polymerizations in CO_2-expanded MMA are given in Table 1. The maximum conversions in bulk polymerizations described in literature are still higher than reported in Table 1 (typically 15% maximum[7]). In this work, we have used a similar ultrasound probe as used for ultrasound-induced bulk polymerizations reported in literature. However, the volume of the reaction calorimeter (1.5 L) is rather large as compared to the typical bulk polymerization reactors (200 mL). Nevertheless, the use of the reaction calorimeter is essential for measuring the heat flow and the overall heat-transfer coefficient. The unfavorable ratio between reactor volume and surface of the ultrasound probe limits the conversion to relatively low values within a realistic time frame. The reaction rates shown in Table 1 and Figure 8b, are a strong indication that indeed high conversions can be achieved using this method.

The majority of the radicals during an ultrasound-induced polymerization reaction are generated by polymer scission. When the reaction conditions are well controlled, these scission reactions are highly reproducible.[23] For this reason, the total configuration of the reactor was exactly kept constant during all the polymerizations as described in the experimental section. Additionally, the conditions inside the reactor (temperature, gas-flow, pressure and stirrer speed) were well controlled by the reaction calorimeter. Because of these precise operating conditions and the reproducibility of the scission reactions, the polymerization reactions are highly reproducible. The inaccuracy of the overall heat-transfer coefficient, the ultrasound intensity and the conversion are approximately 4 W/m^{2}K, 2 W/cm^2 and 0,1%, respectively.

For a proper comparison of the overall heat-transfer coefficients, it is important to use polymers with the same molecular weight, since the viscosity is a function of both the polymer concentration and molecular weight. For this reason, the polymerization in which argon is used as nucleation source (0 bar CO_2), is not given in Figure 7, and a higher amplitude is used at 4.5 bar in order to obtain polymers with similar molecular weights. Figure 7 shows U, which is determined by temperature oscillation calorimetry, as a function of the conversion. It can clearly be seen that the decrease in U is smaller and, hence, the increase in viscosity is lower for higher CO_2 fractions during polymerization. This is a result of the smaller gyration radius of the polymer coils as no precipitated polymer has been found at the final conversion. This positive influence of CO_2 on the solution viscosity has also been seen in the previous section in which no polymerization occurred. To couple the viscosity

Table 1. Results of Ultrasound-Induced Polymerizations of MMA at 20°C and Different CO_2-Pressures (*Reaction started with 1.0 weight% polymer instead of 0.5 weight%)

CO_2-Pressure (bar)	Fraction CO_2	Ultrasound Amplitude (μm)	Ultrasound Intensity (W/cm^2)	Conversion (%)	Initial Rate (mol/m^3 s)	Final Rate (mol/m^3 s)	M_n (kg/mol)
0	0	74	31	3.1	0.037	0.018	110
1.0*	0.02	74	31	3.3	0.019	0.019	471
4.5	0.09	99	102	3.9	0.019	0.040	474
7.0	0.14	74	69	2.5	0.023	0.023	428

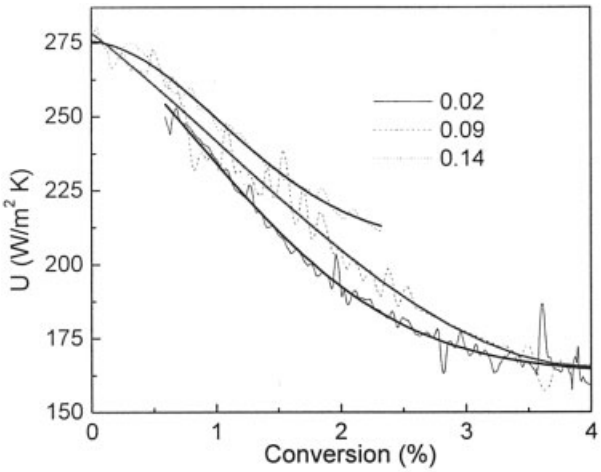

Figure 7. Development of the overall heat-transfer coefficient during the polymerization reactions at three different CO_2 fractions.

to U, the viscosity at 0% and 1.2% conversion at 1 bar CO_2 have been measured, which are $1.0 * 10^{-3}$ and $2.8 * 10^{-3}$ Pa s, respectively. The corresponding overall heat-transfer coefficients are 275 and 225 W/m^2 K (Figure 7) at 0% and 1.2% conversion, respectively. The polymerization reaction with a CO_2 fraction of 0.14, reaches this U-value of 225 W/m^2 K and, hence, the viscosity of $2.8 * 10^{-3}$ Pa s, at a conversion of 1.9%. This theoretically implies that the cavitation intensity and, hence, the radical formation rate at 1.9% conversion and a CO_2 fraction of 0.14 is similar to the radical formation rate at 1.2% conversion, and a CO_2 fraction of 0.02.

The polymerizations in CO_2 show a reaction rate in the same order of magnitude as compared to the bulk experiment at ambient pressure with argon (Figure 8b and Table 1). The initial reaction rates with CO_2 are slightly lower as compared to the bulk experiment. This can originate from the lower polytropic index of CO_2, the higher solubility of CO_2 or the different diffusion properties,[10] due to which the implosion of the cavitation bubbles become less violent. The lower radical formation rate with argon cannot be explained by the change in the number of cavitation bubbles, as less cavitation bubbles are generated with a low-solubility gas (Ar) as compared to a high-solubility gas (CO_2). Although the reaction rates are similar, the polymer produced at 1, 4.5 and 7 bar CO_2-pressure have a much higher molecular weight than the reference polymer in bulk MMA with argon. Kruus et al.[24] found a similar result during an ultrasound-induced polymerization when CO_2 was bubbled through the reaction mixture instead of another gas. A possible reason for the higher molecular weight would be a decrease in the chain transfer rate to monomer, or an increase in the chain transfer rate to polymer. These transfer reactions only influence the produced molecular weight and not the reaction rate. All other reactions, for example, polymer scission, propagation, initiation and termination, affect both the MWD and the polymerization rate.

Figure 8b and Table 1 show that in the experiment with argon the reaction rate decreases, whereas the polymerization rate is constant or even increases when CO_2 is used. This is a result of the viscosity reduction by the anti-solvent behavior of CO_2 at higher polymer concentrations. Consequently, the radical formation rate by cavitation is not decreased when CO_2 is applied. The initial negative influence of CO_2 on the implosion intensity at low polymer concentrations (0.5 wt. %) is, thus, more than compensated at higher polymer concentrations by the anti-solvent effect.

Typically, in ultrasound-induced bulk polymerizations a maximum conversion of approximately 15% can be achieved.[7] At this conversion the collapse of cavitation bubbles is no longer sufficiently strong to generate radicals by ultrasound, due to the high viscosity. The decrease in viscosity by the CO_2 anti-solvent effect implies that higher conversions in CO_2-expanded MMA, as compared to bulk MMA would be possible. Moreover, at higher conversions the polymer will precipitate in the presence of an antisolvent, due to which a constant viscosity is maintained and even higher conversions are expected.

Conclusions

In this work, the influence of the CO_2 fraction on the viscosity and the resulting reaction kinetics of the ultrasound-induced polymerization of MMA have been studied, for which phase equilibrium and density measurements have been performed, as well as polymerization experiments in a reaction calorimeter. The results show that the viscosity is significantly reduced at polymer concentrations at which the coils would overlap in bulk systems without CO_2 present. Due to this antisolvent effect of CO_2, the reaction rate does not decrease, and even increases during ultrasound-induced polymerization in CO_2-expanded MMA, which indicates the possibility to obtain high conversions by ultrasound-induced precipitation

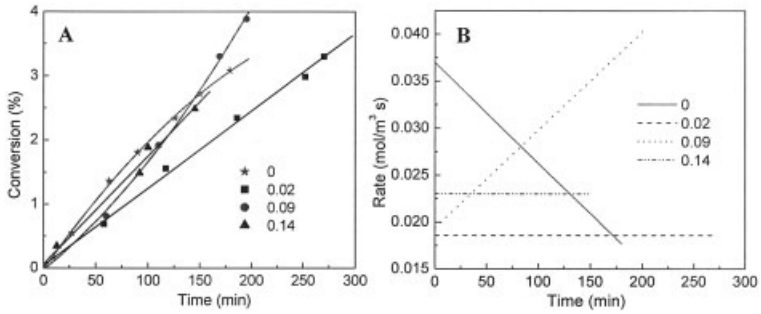

Figure 8. Conversion-time history (A), and reaction rates (B) of ultrasound-induced polymerizations of MMA at various CO_2 fractions.

polymerization. Moreover, the initiator-free and solvent-free polymerization enables a clean and intrinsically safe route to produce polymers with controlled molecular weight.

Notation

μ = viscosity, Pa s
ρ = density, kg/m^3
ω = acentric factor
A = heat-transfer area, m^2
A_{US} = area ultrasound probe, m^2
C_p = specific heat capacity, J/kg K
D = impeller diameter, m
D_0 = outer diameter of reactor, m
D_i = inner diameter of reactor, m
h_i = partial heat-transfer coefficient reactor, W/m^2 K
h_0 = partial heat-transfer coefficient jacket, W/m^2 K
k_i = conductivity of liquid inside reactor, W/m K
k_0 = conductivity of liquid inside jacket, W/m K
k_w = conductivity of reactor wall, W/m K
M_n = number average molecular weight, g/mol
N = stirrer speed, s^{-1}
Nu = nusselt number
Pr = prandtl number
Q = heat flow, W
Re = reynolds number
T_j = jacket temperature, K
T_r = reactor temperature, K
U = overall heat transfer coefficient, W/m^2 K
v = sound velocity, m/s
Z = compressibility

Literature Cited

1. Didenko YT, Mcnamara III WB, Suslick KS. Molecular emission from single-bubble sonoluminescence. *Nature.* 2000;407:877–879.
2. Nguyen TQ, Liang QZ, Kausch H.-H. Kinetics of ultrasonic and transient elongational flow degradation: a comparative study. *Polymer.* 1997;38:3783–3793.
3. Kruus P. Initiation of polymerization with ultrasound. *Ultrasonics.* 1987;25:20–22.
4. Price GJ, West PJ, Smith PF. Control of polymer structure using power ultrasound. *Ultrason Sonochem.* 1994;1:S51–S57.
5. Kuijpers MWA, Kemmere MF, Keurentjes JTF. *Ultrasound-Induced Radical Polymerization.* In: Encyclopedia of Polymer Science and Technology. New York: John Wiley & Sons; 2004.
6. Pestman JM, Engberts JBFN, De Jong F. Sonochemistry: theory and applications. *Recl Trav Chim Pays-Bas.* 1994;113:533–542.
7. Price GJ. Ultrasonically enhanced polymer synthesis. *Ultrason Sonochem.* 1996;3:S229–S238.
8. Canelas DA, DeSimone JM. Polymerizations in liquid and supercritical carbon dioxide. *Adv Pol Sci.* 1997;133:103–140.
9. Kuijpers MWA, Van Eck D, Kemmere MF, Keurentjes JTF. Cavitation-induced reactions in high-pressure carbon-dioxide. *Science.* 2002; 298:1969–1971.
10. Leighton TJ. *The Acoustic Bubble.* London: Academic Press; 1994.
11. Jessop PG, Leitner W. *Chemical Synthesis using Supercritical Fluids.* Weinheim: Wiley-VCH; 1999.
12. Abraham MA, Moens L. *Clean Solvents, Alternative Media for Chemical Reactions and Processing.* Washington: ACS Symposium Series 819;2002.
13. De Loos ThW, Van der Kooi HJ, Ott PL. Vapor-liquid critical curve of the system ethane + 2-methylpropane. *J Chem Eng Data.* 1986;31: 166–168.
14. Benedict M, Webb GB, Rubin LC. An empirical equation for thermodynamic properties of light hydrocarbons and their mixtures. *J Chem Phys.* 1940;8:334–345.
15. Plöcker U, Knapp H, Prausnitz J. Calculation of high-pressure vapor-liquid equilibria from a corresponding-states correlation with emphasis on assymetric mixtures. *Ind Eng Chem Process Des Dev.* 1978;17: 324–332.
16. Kemmere MF, Meuldijk J, Drinkenburg AAH, German AL. Heat transfer in batch emulsion polymerization. *Polymer Reaction Eng.* 2000;8:271–297.
17. Kemmere MF, Kuijpers MWA, Jacobs LJM, Keurentjes JTF. Ultrasound-induced polymerization of methyl methacrylate in liquid carbon dioxide; a clean and safe route to produce polymers with controlled molecular weight. *Macromol Symp.* 2004;206:321–331.
18. Varela de la Rosa L, Sudol ED, El-Aasser MS, Klein A. Details of the emulsion polymerization of styrene using a reaction calorimeter. *J Polym Sci.* 1996;34:461–473.
19. Carloff R, Proß A, Reichert K-H. Temperature oscillation calorimetry in stirred tank reactors with variable heat transfer. *Chem Eng Tech.* 1994;17:406–413.
20. Tietze A, Proß A, Reichert K-H. Temperature oscillation calorimetry in stirred tank polymerization reactors. *DECHEMA Monogr.* 1995; 131:673–680.
21. Xue L, Agarwal US, Lemstra PJ. High molecular weight PMMA by ATRP. *Macromolecules.* 2002;35:8650–8652.
22. Lora M, McHugh MA. Phase behavior and modeling of the poly(methyl methacrylate)-CO2-methyl methacrylate system. *Fluid Phase Equilibria.* 1999;157:285–297.
23. Kuijpers MWA, Iedema PD, Kemmere MF, Keurentjes JTF. The mechanism of cavitation-induced polymer scission; experimental and computational verification. *Polymer.* 2004;45:6461–6467.
24. Kruus P, O'Neill M, Robertson D. Ultrasonic initiation of polymerization. *Ultrasonics.* 1990;28:304–309.

Manuscript received Jun. 2, 2004, and revision received Sept. 14, 2004.